Reaction simulations as a guide to lifetime information from particle-particle correlations

A. Elmaani and John M. Alexander
Department of Chemistry, State University of New York at Stony Brook, Stony Brook, New York 11794
(Received 26 October 1992)

The strength of the final-state interactions between emitted particles depends on the spectrum of time delays between their emissions. Measured correlation functions reflect these interactions, and therefore time-scale information can be obtained by comparisons to associated reaction simulation calculations. We illustrate the sensitivity of the method to the emitter lifetime as well as the attention to several of the details needed for its effective use. Application to one set of data is shown.

PACS number(s): 25.70.z, 21.10.tg

A number of recent studies of intermediate-energy heavy-ion reactions have used particle and or fragment correlation measurements to probe the lifetimes of hot emitter nuclei (see, for example, [1–5]). The general technique is to construct a correlation function from the data and then to make comparisons to model calculations or reaction simulations. Various groups have used different techniques for the construction of these correlation functions, and there is some controversy about the desirability of each technique. Since these correlation functions often reveal rather small effects, it is necessary to stress details in the consistency between the data and the calculations that are used for interpretation. In this study we explore several of these important details by using the reaction simulation code MENEKA [6] along with some data from a recently analyzed experiment [5, 7, 8]. Our objective is to show the sensitivity of the correlation functions to emitter lifetime and to help clarify the need for attention to detail in extracting this information.

A two-particle correlation function $C(P_{\rm rel})$ is normally defined as the ratio of two spectra

$$C(P_{\rm rel}) = A(P_{\rm rel})/B(P_{\rm rel}) \ . \tag{1}$$

The numerator spectrum $A(P_{\rm rel})$ represents the real two-particle coincidence yield, where the relative momentum is defined as

$$P_{\rm rel} = \mu v_{\rm rel} = \mu(v_1^2 + v_2^2 - 2v_1 v_2 \cos\theta)^{1/2} \ . \tag{2}$$

The velocities v_1 and v_2 are the final laboratory velocities of the particles, μ is the reduced mass, and θ is the relative angle of the coincident ejectiles at their detection positions. The denominator spectrum $B(P_{\rm rel})$ is a reference spectrum that is chosen to eliminate or strongly reduce the particle-particle final-state interactions. In an ideal situation, even small deviations of $C(P_{\rm rel})$ from unity will give information on the particle-particle interactions in the exit channel.

While the procedure for constructing the real or correlated spectrum $A(P_{\rm rel})$ is unique, this is not the case for the denominator $B(P_{\rm rel})$. The reference spectrum must be constructed from fictional or false coincidences so as to remove the memory of final-state interactions as much as possible. Two decorrelation methods have emerged as the most commonly used for constructing the reference spectrum, namely, *singles* and *mixing*. Each of these methods presents advantages as well as problems. In order to assess some of the differences between these techniques, we have treated our experimental data in four different ways.

We also implemented three of these decorrelation techniques in the reaction simulation code MENEKA [6]. This allows one to fit an experimental data set in a consistent way. This is an essential point, because consistency in the treatment of the experimental data and the simulation is the first condition to satisfy for any meaningful interpretation. As a test of any of these methods, one would naively hope to produce a flat correlation function for large delay times between particle emissions. In Fig. 1 we develop this test by showing calculated correlation functions for a proton as the trigger particle detected in coincidence with four different sweeper particles, (p, d, t, α). Experimental constraints on acceptance angles and thresholds [5, 7, 8] are respected in the simulations [6].

These calculations have been made for a 312 MeV ^{40}Ar beam colliding with $^{\rm nat}$Ag, assuming that complete fusion has taken place and that the time delay between the emission of two particles is too long (10^{-18} s) for these particles to feel any mutual interaction. These calculations allow one to test if the coincidence spectrum is actually free of any correlations as indicated by comparison to the reference spectrum; if so the correlation will be unity for all values of $P_{\rm rel}$. The calculated correlation functions shown in Fig. 1 were constructed with two different methods (singles and class mixing method to be elaborated later) to test if both reference spectra are identical when the time delays are very large. In both cases, the coincidence (real) spectrum $A(P_{\rm rel}^{\rm real})$ of Eq. (1) is the same. It is only the reference spectrum that is constructed in two different ways.

These calculated correlation functions in Fig. 1 exhibit a trend in the differences between the methods for small relative momenta ≤ 20 MeV/c. As the partner particle of the proton increases in mass p, d, t, α, we see an enhancement above unity for small $P_{\rm rel}$ values in one of the correlation functions (viz. from the singles events). This trend is clearly related to the recoil effect [6, 7]; the deviations vary with the mass of the sweeper particle while the mass of the trigger was unchanged. These observed differences are clearly seen even for large delay time, i.e., "no final-state interaction." When the delay times are

much shorter, this effect is completely obscured by anticorrelations that are generated by Coulomb repulsion. Model calculations that neglect this recoil effect could lead to an overestimation of the average mean lifetime after comparisons to the experimental correlations.

The point of this exercise is to show that model calculations or simulations generally require the inclusion of a three-body final state. Momentum conservation involves consideration of the emitter nucleus as well as the emitted particles. Other isotropically emitted particles that are not detected play a very small role since their effects are averaged over all angles. Now let us turn from simulation to experimental data.

As stated above, we have compared experimental correlation functions constructed in four different ways; let us first briefly describe these techniques for building the reference spectra. (1) Singles enabling (SE): The relative momentum is calculated from a pair of particles that originate from two separate singles-enabled events. (2) Cross beam (CB): To improve on the singles, where one may be selecting reaction mechanisms that are different from those in coincidence, we create a new set of pseudo "singles events" from coincidence events measured at large relative angles. The intent here is to eliminate any interaction but still to select equivalent types of reactions as those for the real spectrum. (3) Class mixing (CM): In this case the two particles that are used for calculating $P_{\rm rel}^{\rm fake}$ are taken from two successive events that satisfy the same relative geometrical positions. In other words reference detector pairs are designated for each equivalent detector pair. The conditions used for creating these reference pairs and consequently the coincidence class (or group of detector pairs that have similar geometry) are the relative azimuthal angles $\Delta\Phi$ and the absolute polar angles θ. (4) Event mixing (EM): This is a simplified version of the (CM) method, where no geometrical restrictions or conditions are applied for the mixing. Each event produces one particle to be coupled with a partner particle originating from the following event to produce $P_{\rm rel}^{\rm fake}$.

We have applied these four techniques to experimental data for all pairs of particle-particle correlations, but for the purpose of illustration, we show here only two cases (^{1}H-^{1}H and ^{4}He-^{4}He). The first case is shown in Fig. 2; these ^{1}H-^{1}H correlations are representative of the cases where no unstable fragment breakup is known to compete with the evaporation process. At the low energy (312 MeV, bottom figure), the anticorrelation is quite weak; thus one can hardly see any differences among the four symbols corresponding to the four choices for the reference spectrum. At the higher energy (680 MeV, top figure), in the region of interest for these small-angle correlations (i.e., small $P_{\rm rel}$), we can see that the singles (square symbols) produce the lowest points or the strongest anticorrelations. These larger deviations from unity can be attributed to a slightly more complete decorrelation in background spectrum, $B(P_{\rm rel}^{\rm fake})$ or the denominator in Eq. (1).

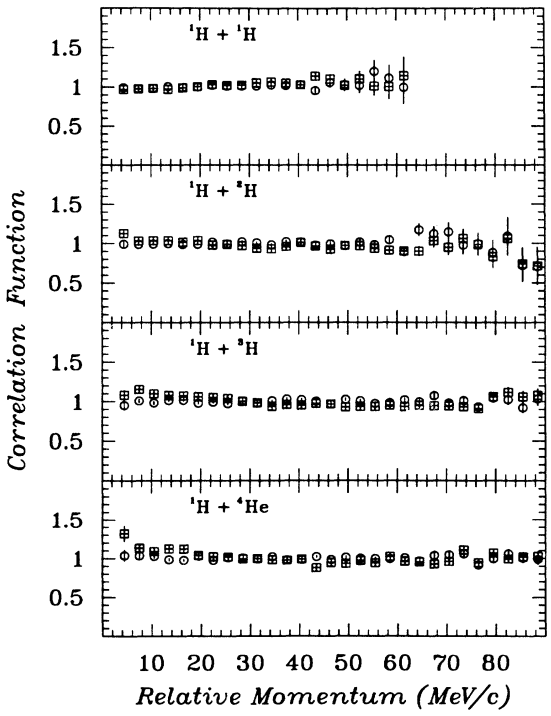

FIG. 1. Particle-particle correlation functions calculated [6] for ^{1}H in coincidence with ^{1}H, ^{2}H, ^{3}H, and ^{4}He particles. Large mean lifetimes ($\tau = 10^{-18}$ s) were used throughout. (⊞) singles; (○) mixed events.

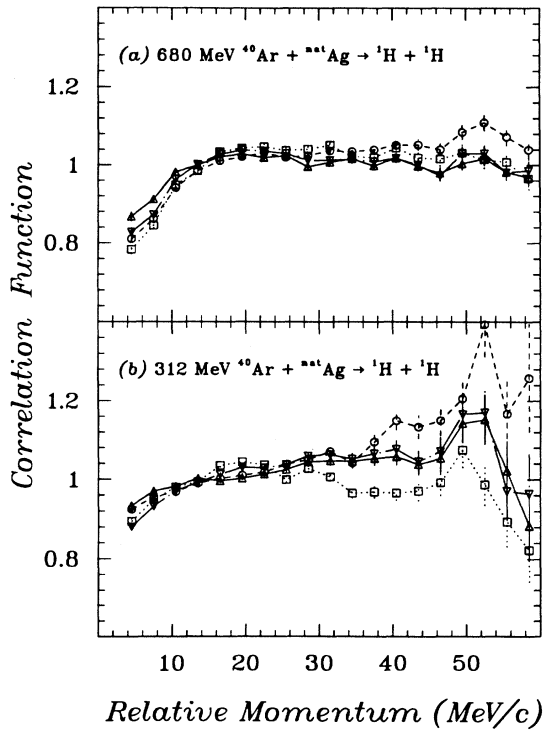

FIG. 2. Four experimental correlation functions [8], constructed by changing only the reference spectrum from (singles, cross beam, class mixing, and event mixing), for ^{1}H-^{1}H pairs from two bombarding energies; (a) 680 MeV and (b) 312 MeV ^{40}Ar+ ^{nat}Ag. (△) class mixing; (□) singles; (○) cross beam; (▽) event mixing.

These results can be easily confirmed and emphasized by examination of the ^{4}He-^{4}He correlation functions as shown in Fig. 3. The relative peak heights in these correlations are determined by how well the reference spectrum "forgets" that a number of the α particles originate from ^{8}Be fragment breakup. For pairs such as α-α, the dominant feature of the correlations is produced by the breakup of a ^{8}Be fragment to give a peak in the real $P_{\rm rel}$ spectrum and hence in the correlation function [9]. It is clear for this case that the efficiency of the decorrelation method can be evaluated by how well the $P_{\rm rel}$ values for the particle pairs are redistributed in the generation of the reference spectrum. If all traces of the ^{8}Be breakup peak in the real coincidence spectrum $A(P_{\rm rel})$ are lost in the fake coincidence spectrum $B(P_{\rm rel})$ then the peak in the correlation function will be most clear. Any residual peak in $B(P_{\rm rel})$ will diminish the resultant peak in the correlation function.

From the observed differences in the measured correlation functions shown in Fig. 3, we can classify the four methods by a comparison of their peak heights in the region for ^{8}Be$_{\rm g.s.}$ breakup (i.e., $\approx$ 19.5 MeV/c). We find that the singles and the cross beam coincidence selection techniques give stronger peaks, and thus their reference spectra must be more decorrelated than for either of the mixing techniques.

We do have to point out, at this point, that these observations do not imply that one method is, in general, any better that another one. A consistent treatment of experimental and calculated correlation functions will compensate for the differences between these methods [6]. However, to justify a particular choice of method, one should consider all aspects involved in the way the reference spectrum is constructed. To elaborate this idea we turn now to simulation calculations for a further analysis of these methods for generating the reference spectra.

Reaction simulations give a way to explore the effect of delay time (in this case the most important parameter) on the reference spectrum. The assumption of this simulation is that the final-state interactions drive the correlations, and since one wishes to see very small effects, they can be enhanced by the use of a correlation function. Hence it is important to check and to evaluate if the reference spectrum is indeed independent of the final-state interactions of interest. That is, if the real coincidences are affected by variations in the emission time delays, the fake coincidences should, in the ideal situation, be free of these variations.

To explore and test for such effects on the construction of the reference spectrum, we use event by event simulations of experimental data. It is only through simulation calculations that one can develop a pattern for these changes, when the delay time is varied. We have adopted this approach for one case, to explore these variations by changing the mean lifetime over the time scale range of 10^{-20} to 10^{-22} s.

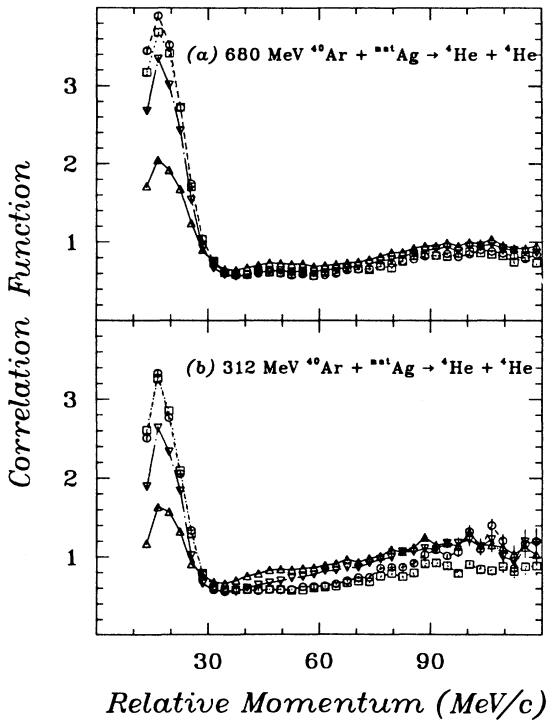

FIG. 3. Four experimental correlation functions [8], constructed by changing only the reference spectrum from (singles, cross beam, class mixing, and event mixing), for ^{4}He-^{4}He pairs from two bombarding energies; (a) 680 MeV and (b) 312 MeV ^{40}Ar+ $^{\rm nat}$Ag. (Δ) class mixing; ($\Box$) singles; ($\circ$) cross beam; (∇) event mixing.

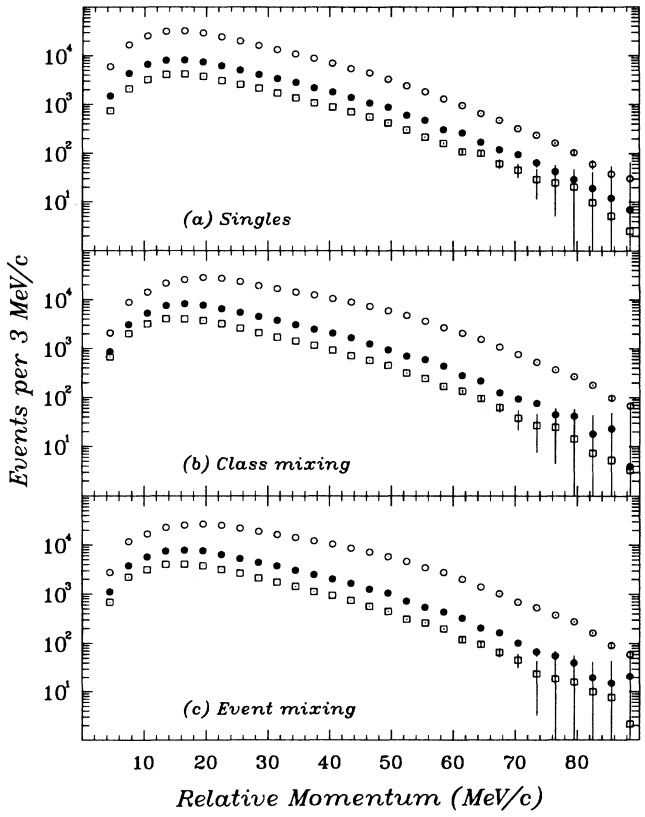

FIG. 4. Illustration of the change in the reference spectrum calculated from (a) singles, (b) class mixing, and (c) event mixing for ^{1}H-^{1}H pairs for 680 MeV ^{40}Ar + $^{\rm nat}$Ag. ($\Box$) $\tau_{p-p} = 10^{-20}$ s; ($\bullet$) $\tau_{p-p} = 10^{-21}$ s; ($\circ$) $\tau_{p-p} = 10^{-22}$ s.

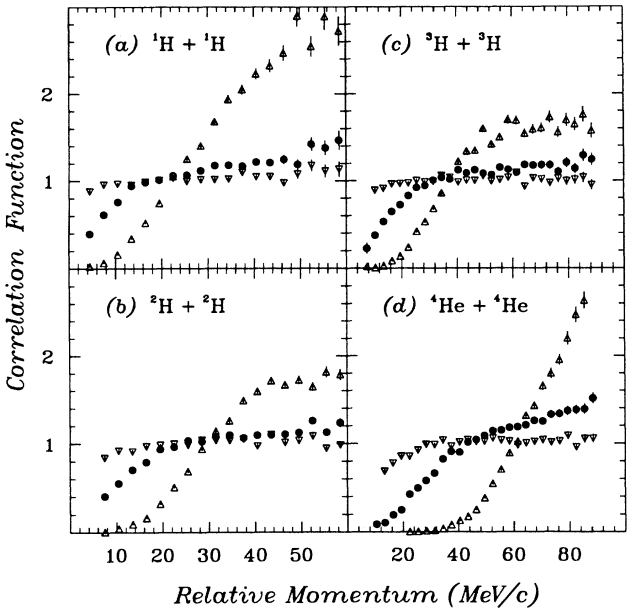

FIG. 5. Calculated correlation functions (singles reference spectra) for ^{1}H-^{1}H, ^{2}H-^{2}H, ^{3}H-^{3}H, and ^{4}He-^{4}He pairs for three different mean lifetimes τ of 10^{-22}, 10^{-21}, and 10^{-20} s. τ = 10^{-22} s; ($\triangle$); 10^{-21} s ($\bullet$); 10^{-20} s (∇).

Results of such calculations are shown in Fig 4 for ^{1}H-^{1}H correlations from the reaction 17A MeV ^{40}Ar + ^{nat}Ag. Three mean lifetimes, τ_{pp} = 10^{-20}, 10^{-21}, and 10^{-22} s, were used to search for effects on the reference spectrum. For reference spectra from singles, as shown in Fig. 4(a), we can see that the three calculated reference spectra are essentially the same over the whole extent of the relative momentum spectrum (the three calculated curves were arbitrarily normalized). But in the second case [class mixing shown in Fig. 4(b)], one can clearly see that, especially for very small relative momenta (below 20 MeV/c), the three curves show different shapes. Similar trends are observed in Fig. 4(c) (event mixing) but on a lesser scale. This leads us to conclude that in the last two cases changes in the lifetime have affected the fake coincidences, hence producing reference spectra that are not as free from the time-driven correlations. This result gave us encouragement to select the singles method for our reference spectra [8]. With this choice for the reference spectrum we now show some simulations that illustrate the effect of emitter lifetime on the correlation function.

The code MENEKA provides many input parameters to allow one to test for the role of many physical effects. It is beyond our scope here to illustrate most of them. However, we would like to show the sensitivity of the calculated correlation functions to the delay times between particles for typical light charged particle correlations. In the context of this model framework, these delay times are the major driving force for the correlation functions.

Interpretation of experimental particle-particle correlations can be made only via comparisons to calculated correlations from a simulation code. The purpose of these comparisons is to serve as a test for this all-important role of the spectrum of particle emission times. In Fig. 5 we show calculated correlation functions for four pairs of particles generated in the reaction 680 MeV ^{40}Ar + ^{nat}Ag. For each case a normalization of the P_{rel} spectra has been made by demanding equal area (or event numbers) for $A(P_{rel})$ and $B(P_{rel})$. Some other workers have normalized by demanding that $A(P_{rel})/B(P_{rel})$ be unity for "large P_{rel}." This latter procedure can lead to ambiguities in the selection of large P_{rel} as shown in Fig. 5.

The input for these calculations has been taken from the detector properties used in this experiment and from measured particle spectra. The major trend is an anticorrelation at low values of P_{rel} which strengthens with decreasing lifetime. For the longest lifetimes (τ = 10^{-20} s) the anticorrelation is barely perceptible for ^{1}H-^{1}H pairs, but becomes clearer for ^{2}H-^{2}H, ^{3}H-^{3}H, and ^{4}He-^{4}He pairs. Note that only the first bin (P_{rel} = 4.5 MeV/c) of this correlation function deviates from unity. For P_{rel} values greater than 4.5 MeV/c the correlation function is unity within the statistical fluctuations. For much shorter lifetimes the anticorrelation hole is very deep and a broad peak arises at rather large P_{rel} values. With decreasing lifetime for a given particle pair the anticorrelation grows due to a decrease in the flight distance for the first particle before the birth of the second. Similarly the ^{2}H-^{2}H pairs are more strongly correlated than the ^{1}H-^{1}H pairs (for a fixed τ) because the ^{2}H particles have slower velocities and, therefore, smaller flight paths. This trend is extended by examination of correlation functions for ^{2}H-^{2}H pairs as compared to ^{3}H-^{3}H for the same average mean lifetime τ. The ^{4}He-^{4}He pairs are even more strongly correlated because of their larger charge product (Z_1Z_2); unfortunately experimental correlations for ^{4}He-^{4}He pairs do not exhibit the same trends due to the presence of strong peaks from ^{8}Be breakup into two α particles [8, 9].

By comparison of calculated curves like these to experimental data, one can hope to test the range of mean time intervals between particle emissions (or decay lifetimes) in this region of $10^{-22} - 10^{-20}$ s. If the emission time delays are extremely short, e.g., $\tau \leq 10^{-22}$ s, one can also expect the intrinsic nuclear sizes to play a role in the correlations [7, 10].

[1] D. Ardouin (ed.), *Proceedings of Corinne 90*, An International Workshop on Particle Correlations and Interferometry in Nuclear Collisions, Nantes, France, 1990 (World Scientific, Singapore, 1990).
[2] P. A. DeYoung *et al.*, Phys. Rev. C **39**, 128 (1989).
[3] D. H. Boal *et al.*, Rev. Mod. Phys. **62**, 553 (1990).
[4] J. Pochodzalla *et al.*, Phys. Rev. C **35**, 1695 (1987).
[5] A. Elmaani *et al.*, Phys. Rev. C **43**, R2474 (1991).
[6] A. Elmaani *et al.*, Nucl. Instrum. Methods, Phys. Res. A **313**, 401 (1992).
[7] A. Elmaani, Ph.D. thesis, State University of New York at Stony Brook, Stony Brook, New York, 1991.
[8] A. Elmaani *et al.*, Stony Brook report, 1992.
[9] M. S. Gordon *et al.*, Phys. Rev. C **46**, R1 (1992)
[10] J. M. Alexander *et al.*, Stony Brook report, 1992.